

# TEMPORAL IMAGING WITH THE UP-CONVERSION TIME MICROSCOPE

C. V. Bennett, R. P. Scott, and B. H. Kolner

Electrical Engineering Department  
University of California, Los Angeles

Box 951594  
Los Angeles, CA 90095-1594

# Temporal imaging with the up-conversion time microscope

C. V. Bennett, R. P. Scott, and B. H. Kolner

Electrical Engineering Department, University of California, Los Angeles  
Box 951594, Los Angeles, CA 90095-1594

Phone: (310) 825-8899 FAX: (310) 206-8495 email: bennett@ee.ucla.edu

## ABSTRACT

We have demonstrated a temporal imaging system with a novel time lens which magnifies 100 Gb/s optical data by a factor of twelve. The function of a time lens is to impart a quadratic phase modulation or linear frequency sweep to the waveform under study. Our approach to achieving time lens action is to up-convert the waveform under study using a linearly swept pump, thus imparting a linear frequency sweep to the waveform. This technique allows for much greater frequency sweep rates and hence shorter focal times than can be obtained with electro-optic modulators. Additionally, the increased bandwidth that can be obtained optically instead of electro-optically should result in higher resolution in a temporal imaging system.

**Keywords:** temporal imaging, time lens, time microscope, ultrashort light pulses, ultrafast phenomena.

## 1. INTRODUCTION

The direct measurement of ultrashort light pulses and waveforms is limited by current technology to several picoseconds resolution. New techniques for improving resolution generally concentrate on faster photodetectors and sampling electronics which are, of course, very important and form the foundation for all high speed optical measurements. There is, however, the possibility of modifying the optical waveform before it is detected by effectively slowing it down to a speed that is within the capabilities of state-of-the-art instrumentation. This is the approach that we have been developing and it is called “temporal imaging” in direct analogy with spatial imaging.

The objective in both spatial and temporal imaging is to expand or compress a field or waveform and preserve its overall profile, be it a function of space or of time. The technology of the former has been around for several centuries and is familiar to most everyone. The technique of temporal imaging is based on a one-to-one analogy between the processes that occur in the spatial case and those that occur in the temporal case. For example, the phenomenon of diffraction has a dual in the equation that describes the dispersion of light pulses in dielectric media.<sup>1-3</sup> In addition, there is a one-to-one correspondence between the action of a conventional lens and a quadratic phase modulation applied to a time waveform. When these simple elements are combined in proper measure, a system is formed which can magnify or demagnify optical time waveforms.<sup>2,4-7</sup> This is the essence of temporal imaging.

## 2. TEMPORAL IMAGING

From the space-time duality mentioned above, we can prescribe an arrangement of dispersion and quadratic phase modulation as shown in Fig. 1 to realize a temporal imaging system. The input and output dispersions play the same role in the time domain as do object and image distances (diffraction) in the spatial domain. When a signal propagates a distance  $\xi$ , through a medium characterized by normalized group dispersion  $d^2\beta/d\omega^2$ , the phase filtering introduced in the frequency domain is quadratic in frequency  $\omega$  and linear with the net dispersion  $\xi(d^2\beta/d\omega^2)$ . After propagating through the input dispersion, the waveform next encounters a quadratic phase modulation, which acts as a time lens and is characterized by the focal time  $f_T \equiv \omega_o/(d\omega/dt)$ , where  $\omega_o$  is the mean optical carrier frequency out of the lens and  $d\omega/dt$  is the linear chirp rate imparted by the lens. If the proper input dispersion, time lens strength, and output dispersion are cascaded in accordance with the temporal imaging condition<sup>7</sup>

$$\frac{1}{\xi_1 \frac{d^2\beta_1}{d\omega^2}} + \frac{1}{\xi_2 \frac{d^2\beta_2}{d\omega^2}} = -\frac{\omega_o}{f_T} = -\frac{d\omega}{dt}, \quad (1)$$

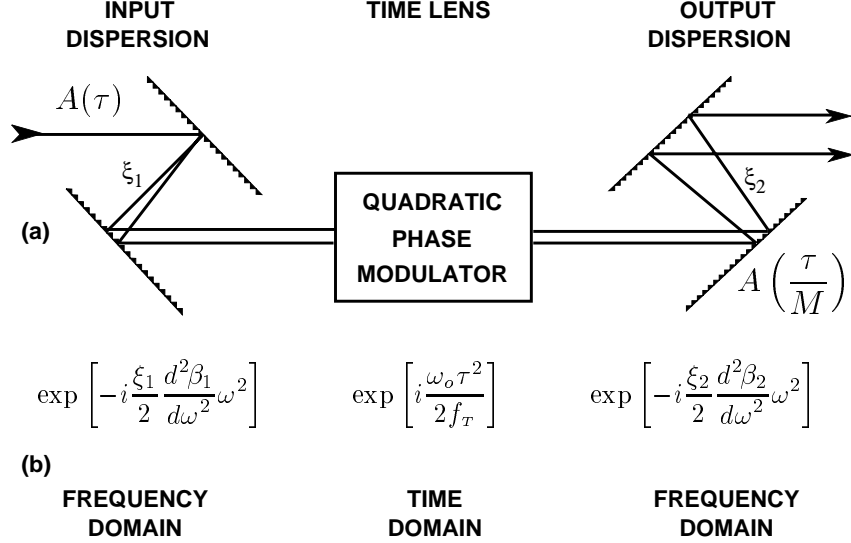


**Figure 1.** (a) Schematic diagram of a temporal imaging system. Input and output dispersions play the role of free space diffraction while quadratic phase modulation in time acts as a time lens. The output waveform, a temporal image, is a magnified replica of the input waveform. (b) Analysis is carried out by cascading the three processes: input dispersion (quadratic phase filtering in the frequency domain), time lens (quadratic phase modulation in time), output dispersion.

then a temporally scaled and time reversed replica of the input waveform will be produced at the output. This temporal image will have a magnification

$$M = -\frac{\xi_2 \frac{d^2\beta_2}{d\omega^2}}{\xi_1 \frac{d^2\beta_1}{d\omega^2}}. \quad (2)$$

The performance of any imaging system, be it spatial or temporal, is limited by the  $f^\#$  of the lens. In the time domain,  $f^\#$  is defined as the focal time-to-temporal aperture ratio, which simplifies to the inverse fractional bandwidth  $\omega_o/\Delta\omega$ , where  $\Delta\omega$  = total bandwidth induced by the lens.<sup>8</sup> The conventional technique for realizing a time lens is by using an electro-optic phase modulator. The modulation bandwidth  $\Delta\omega = \Gamma_o\omega_m$  where  $\Gamma_o$  = peak phase deviation and  $\omega_m$  = modulation frequency. Technological considerations limit the modulation bandwidth producible with electro-optic time lenses and therefore limit the performance of these lenses. Nonetheless, they have been used to successfully demonstrate active pulse compression and temporal imaging.<sup>9–13</sup>

We have been developing an alternative method of obtaining strong time lens action that does not rely on electro-optic modulation. Since the objective of a time lens is to impart a large linear chirp (quadratic phase) and large fractional bandwidth to the dispersed input signal, we use sum frequency generation in a nonlinear crystal to impart the frequency sweep of a highly chirped pump to the input signal.<sup>14,15</sup> Much larger chirp rates and fractional bandwidths can be obtained in this manner than with current electro-optic modulator technology. There is a price to be paid, however, in the inefficiency of the up-conversion process. It is also important to note that because  $\omega_o$  is the mean optical carrier frequency out of the time lens there is an increase in the focal time and  $f^\#$  due to the up-conversion process.

A schematic diagram of our up-conversion temporal imaging system is shown in Fig. 2. The test waveform is a 100 Gb/s four bit digital word and passes through a diffraction grating-pair dispersive delay line which is equivalent to the object-to-lens distance in a conventional spatial imaging setup. The dispersed test waveform is combined with

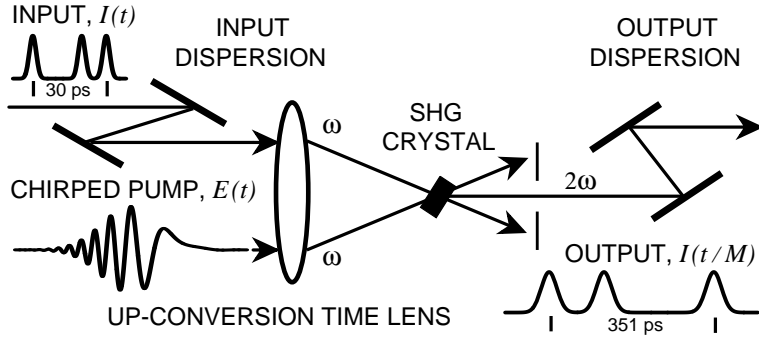


**Figure 2.** Schematic diagram of the up-conversion time microscope system. The time lens is achieved by sum frequency generation of the dispersed input signal  $I(t)$  and a chirped pump  $E(t)$ . Input and output dispersions were achieved using two pairs of diffraction gratings. The measured temporal image of the 100 Gb/s **1101** input test pattern was a **1011** waveform at 8.5 Gb/s.

a linearly chirped pump in a second harmonic crystal cut for noncollinear second harmonic generation. The signal that emerges at  $2\omega$  is a frequency doubled replica of the dispersed input waveform with a linear chirp imparted to it. Finally, the up-converted signal passes through another grating-pair dispersive delay line which functions as the lens-to-image propagation distance. The resulting waveform is a magnified and time-reversed replica of the input digital word and is measured with a standard high-speed photodiode and sampling oscilloscope. Since the goal of this imaging system was to magnify waveforms that were not directly observable with off-the-shelf instruments, we consider the system a “time microscope.” With this brief description of the operation of the time microscope in mind, we now proceed to a more detailed discussion of the various components of the system.

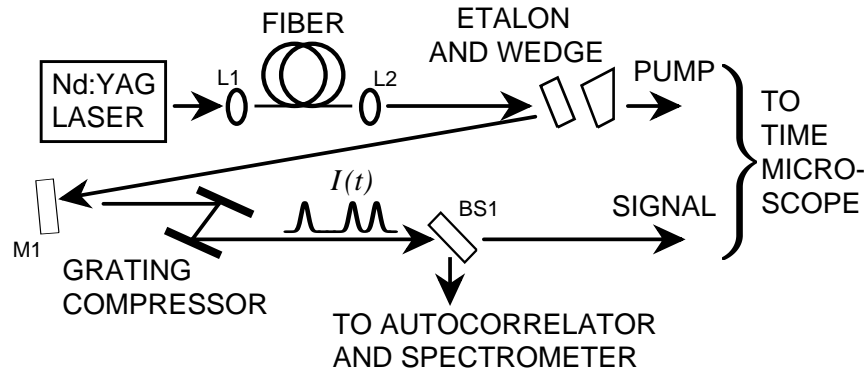


**Figure 3.** Schematic diagram showing the arrangement for generation of the 100 Gb/s **1101** test pattern (SIGNAL) and the chirped pump for the up-conversion time lens (PUMP).

### 3. SYSTEM DETAILS

In order to test the system, a high speed test waveform was needed. Since digital optical pattern generation is not easily accomplished at 100 Gb/s, and certainly not commercially available, we resorted to the simple expedient of using the reflections from air-glass interfaces to appropriately space picosecond pulses in the form of a binary test pattern. The test pattern generator is shown in Fig. 3. The source is a modelocked Nd:YAG laser which produces 71 ps pulses at 80 MHz repetition rate. These pulses are coupled into 70 m of single mode polarization maintaining fiber and emerge chirped and spectrally broadened due to self-phase modulation with a bandwidth of 620 GHz. The peak power output of 67 watts was limited by the onset of stimulated Raman scattering. The chirping of the pulses in the fiber serves two purposes. First, we needed to create reasonably short pulses from the initial pulsewidth of 71 ps. Calculations indicated that 70 m of fiber would produce enough bandwidth to compress the pulses to the 1-2 ps range. Second, some fraction of the uncompressed linearly chirped pulses could serve the dual purpose of the

pump for the up-conversion time lens. Thus, upon exiting the fiber, the chirped pulses pass through a 1 mm thick uncoated fused silica etalon and then through an uncoated  $2^\circ$  fused silica wedge. The reflections off the front and back surfaces of the etalon combine collinearly with the reflection off the front surface of the wedge at a very shallow angle with respect to the input beam. This reflected beam is now composed of three overlapping chirped pulses. The first two are separated by a measured round-trip transit time of 9.2 ps in the etalon. The third pulse comes from the reflection off the front surface of the wedge which is positioned behind the etalon so that the pulse arrives 30 ps after the first pulse. The beam is finally passed through a pair of 1700 1/mm diffraction gratings adjusted to optimally compress the chirped pulses to an autocorrelation width of 2.1 ps. The pulse sequence forms the digital word **1101**.

The orientation of the gratings, the normalized group delay dispersion  $d^2\beta/d\omega^2$  and the distance  $\xi$  between them result in a net dispersion of  $2\pi\xi(d^2\beta/d\omega^2) = -90$  fs/GHz. Notice that the gratings could have been placed ahead of the etalon-wedge pair or in the path of the reflected beam since these two groups form a linear system. However, since 84% of the power is transmitted through the etalon-wedge pair, we chose to use that power in the form of uncompressed pulses as our chirped pump. Thus the gratings were used to compress the *reflected* pulses.

The net dispersion of the compression gratings (Fig. 3) that produces ideally compressed pulses tells us the pump chirp rate<sup>16</sup> since the grating pair forms a matched filter for the linear chirp. Another way to see this is to use the imaging equation (1) and assume that the object is located at infinity ( $\xi_1 = \infty$ ). The pump chirp rate is then simply

$$\frac{df}{dt} = -\frac{1}{2\pi\xi \frac{d^2\beta}{d\omega^2}} = 11.1 \text{ GHz/ps.}$$

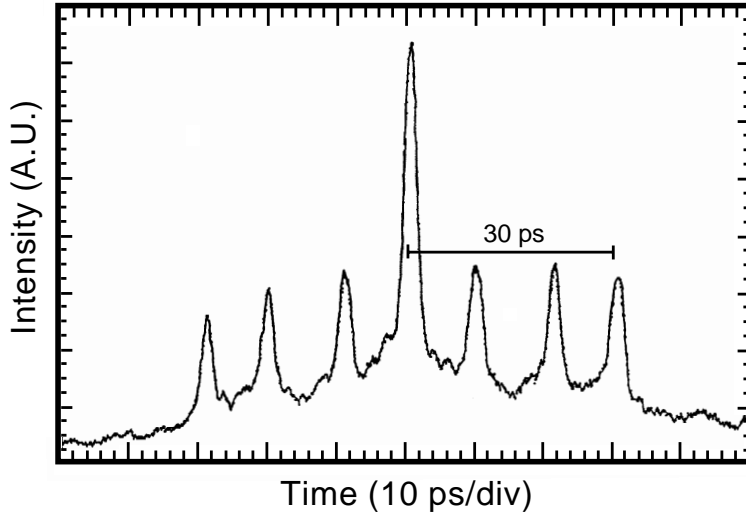


**Figure 4.** Autocorrelation waveform of the **1101** 100 Gb/s optical word used as a test pattern for the time microscope.

The autocorrelation of the test waveform produced from this system is shown in Fig. 4. The pulse-to-pulse spacing is seen to be about 10 ps, demonstrating 100 Gb/s data rate. The amplitude of the main lobe compared to the side lobes does not show the expected 3:1 ratio. We believe that this is due to unequal pulse amplitudes within the word as well as the small ratio of pulse spacing to pulse width.

With the test waveform and chirped pump prepared as in Fig. 3, the two beams are sent into the up-conversion time microscope of Fig. 2. The input test word is first passed through a grating-pair dispersive delay line which acts as the object-to-lens distance. The output beam from the delay line is combined with the chirped pump in a  $\text{LiIO}_3$

crystal cut for noncollinear second harmonic generation. The up-converted signal at 532 nm is simply the dispersed test pattern with a linear frequency sweep imparted to it and is precisely what is desired for time lens action, albeit at a new carrier frequency. Finally, the up-converted waveform passes through another pair of diffraction gratings which serve as the lens-to-image distance. The waveform is now time reversed and magnified.

The net dispersion of the delay lines are chosen to simultaneously satisfy the imaging equation (1) and the magnification equation (2). We chose a magnification  $M = -10$ , which, in combination with the known chirp rate of the pump yields two equations in two unknowns. The input gratings have a groove density of 1700 1/mm and are adjusted for a net dispersion of  $2\pi\xi_1(d^2\beta_1/d\omega^2) = -98.7$  fs/GHz. They are used in double-pass with a vertical translation prism and have a single-pass spacing of 28.4 cm. The input angle was set to  $68^\circ$  with respect to the normal of the grating face. The output gratings have a groove density of 3350 1/mm (optimum for 532 nm) and are adjusted for a net dispersion of  $2\pi\xi_2(d^2\beta_2/d\omega^2) = -987$  fs/GHz. They are also used in a double-pass configuration and have a single pass spacing of 311.4 cm. The input angle was set to  $57.5^\circ$  with respect to the normal.

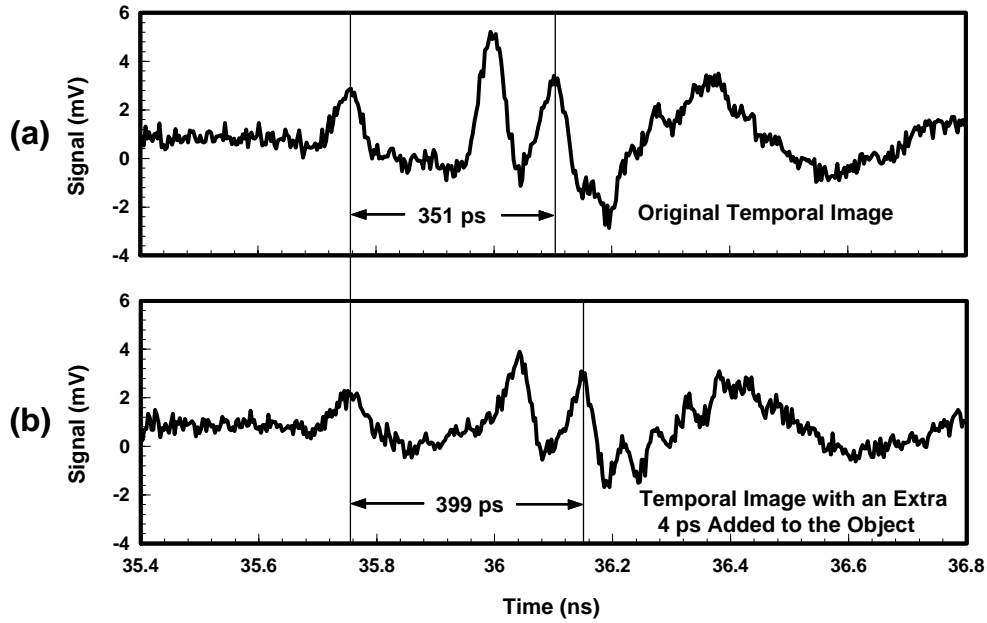


**Figure 5.** Measured temporal images. (a) The original temporal image is a **1011** pattern with 351 ps from first to last pulse, a magnification of  $M = -11.7$ . (b) When a 4 ps change was made to the input signal the new temporal image showed a corresponding 48 ps increase.

#### 4. RESULTS

The temporal image was measured with a high-speed photodiode and 34 GHz sampling oscilloscope. Because of low conversion efficiency to the second harmonic in the time lens and 20% throughput efficiency of the output dispersive network, electronic amplification of the detected signal was necessary. Two amplifiers with a total gain of 35 dB from 2-20 GHz were used. Fig. 5a shows the measured image. It is a **1011** pattern with 351 ps between the first and last pulse. The waveform is a time-reversed and expanded replica of the input demonstrating a magnification  $M = -11.7$ . The ringing following the bit pattern and the increased width of the pulses is due to the limited bandwidth of the amplifiers.

To verify the magnification as well as the overall validity of the time microscope, we modified slightly the input word and observed the change in the image. The etalon was moved  $600 \mu\text{m}$  further away from the wedge, moving the first two pulses of the test pattern 4 ps earlier in time. This resulted in an additional 48 ps delay of the last two pulses of the temporal image (the change from Fig. 5a to Fig. 5b), indicating a magnification of  $M = -12$ . The arrival time of first pulse (originating from the wedge) and the separation between the pulses from the etalon surfaces were unchanged, as expected.

## 5. DISCUSSION

The system was designed for a magnification of  $M = -10$  and yet both measurements described above yielded actual magnifications of  $M \approx -12$ . A potential problem that looms in this kind of a system is inaccuracy in determining that the system is actually temporally focused. The reason for this is twofold. First, the temporal depth of field of this system is very large, thus very large changes in dispersion are required to make any significant change in the output optical pulse widths. Assuming that the system was originally perfectly focused, a change in the physical separation of the output gratings of 1.6 m would only cause the output optical pulse widths to increase by  $\sqrt{2}$ . The second problem is the impulse response of the electronics. The limited bandwidth of the amplifiers broadened the electrical impulse response to 43 ps, approximately three times the expected optical pulse width out of the time microscope, thereby obscuring the true pulse width. Therefore, the magnification was determined by the ratio of output pulse separations to input pulse separations, not the ratio of pulse widths. To understand the source of the 20% error in the system magnification we must understand how magnification varies in the nearly focused regime.

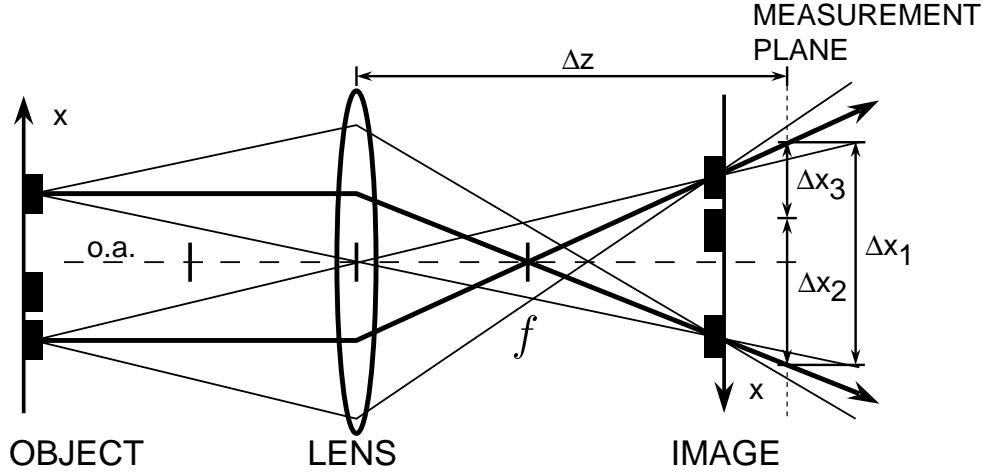


**Figure 6.** A spatial imaging system showing the consequences of observing in a plane removed from the image plane (misfocusing). Separations ( $\Delta x_n$ ) grow linearly with the distance  $\Delta z$ .

Review for a moment the spatial imaging system shown in Fig. 6, having an object made up of three spots. Think of these spots as point sources or gaussian beams with their beam waists at the object plane. The propagation of the light is depicted by a bundle of rays in the figure. The lens redirects the light through the focal point and forms an image in the image plane. If we were to make an observation at a measurement plane  $\Delta z > f$  away from the lens, we would observe blurred spots whose separation  $\Delta x$  increases as  $\Delta z$  is increased. The spots focus forming an image in the image plane and then blur again. The separations of the spot centers increase linearly with  $\Delta z$  and depend inversely on the focal length  $f$ , as given by

$$M = \frac{\Delta x_{out}}{\Delta x_{in}} = 1 - \frac{\Delta z}{f}. \quad (3)$$

Even though the spot size is a minimum in the image plane, the separation of the spots always increase when  $\Delta z$  is greater than  $f$ . In a temporal imaging system, the pulses measured on the oscilloscope separate in time as they are measured with increasing output dispersions. The temporal separation of the pulses at the output as a function of the output dispersion is

$$\begin{aligned}
M &= \frac{\Delta t_{out}}{\Delta t_{in}} = 1 + \frac{\tau_{g2}}{f_T} \\
&= 1 + \xi_2 \frac{d^2\beta_2}{d\omega^2} \frac{d\omega}{dt},
\end{aligned} \tag{4}$$

where  $\tau_{g2}$  is the group delay through the output dispersive delay line. The change in sign between the spatial (3) and temporal (4) magnification equations is due to a fundamental difference between paraxial diffraction and narrow band dispersion which is explained in detail in Ref. 7. Eq. (4) yields the same results as Eq. (2) only at the image plane where Eq. (1) is satisfied. At any other output dispersion the magnification depends linearly on the chirp rate of the time lens and is independent of the input dispersion. Therefore a measurement of pulse separation at the output as a function of output dispersion could be used to determine the chirp rate of the time lens, assuming that the output dispersion is known accurately.

Although this discussion is based on a geometric optics point of view, Eq. (4) can also be understood by examining the optical carrier frequency and group delay of the pulses traveling in a temporal imaging system. The three pulses of the temporal object arrive at the time lens broadened due to the input dispersion but with the same temporal separation as in the object plane since they have the same carrier frequency and thus the same group delay through the input dispersion. While imparting a linear frequency sweep to the dispersed input, the time lens causes a change in optical carrier frequency between pulses of  $\Delta t_{in}(d\omega/dt)$ . Each pulse at a different carrier frequency experiences a different group delay through the output dispersion resulting in Eq. (4).

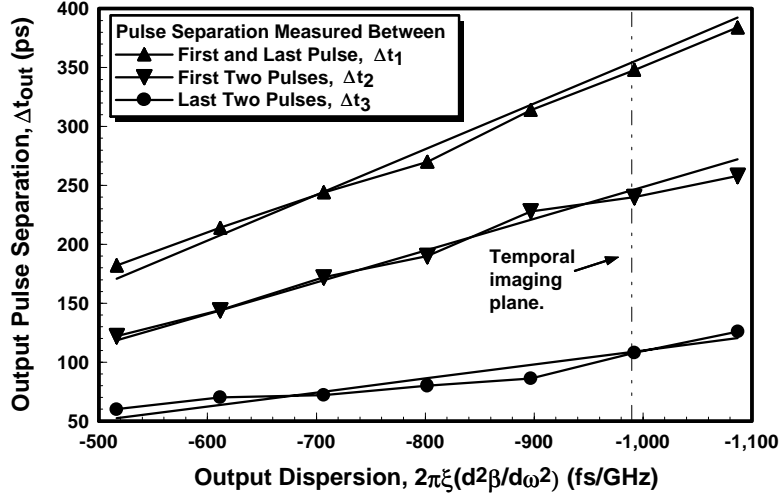


**Figure 7.** Measured separations of the pulses in the output waveform as the output dispersion is varied. Fitting the data to Eq. (4) gives a chirp rate of  $df/dt = 12.95$  GHz/ps and the three straight lines through the data points.

The data points in Fig. 7 are the measured time delays (separations) at the output for the three pulse pair combinations and varying output dispersions. Input pulse separations are given in Sec. 3. Assuming that the output dispersion was known exactly, a chirp rate was calculated for each data point using Eq. (4). The average chirp rate for this ensemble is  $df/dt = 12.95$  GHz/ps instead of the 11.15 GHz/ps determined earlier. The three straight lines in Fig. 7 were plotted using the average chirp rate and illustrate the quality of the fit to Eq. (4). The time lens is therefore stronger than originally expected. This could be due to errors in determining the dispersion of the compression gratings in Fig. 3 or in the human judgment made in setting them to what looks like an optimally compressed autocorrelation trace.

Of course there is uncertainty in the magnitude of the output dispersion as well. In taking the data shown in Fig. 7 the input angle was kept fixed and the grating separation  $\xi$  was changed to vary the output dispersion. The

normalized dispersion  $d^2\beta/d\omega^2$  is a highly nonlinear function of input angle and when set for large dispersion a small error in the input angle can cause large changes in the resulting dispersion. If we assume that the original chirp rate is correct, a  $0.5^\circ$  error in the setting of the input angle to the first grating would account for 9% of the error in the measured magnification. Other possible sources of error include inaccuracy in measuring the grating separation and determining the parallelism of the grating pair.<sup>17</sup>

## 6. CONCLUSION

We have demonstrated a new time lens technique and its use in temporal magnification of ultrafast optical data. This new technique is based on sum frequency generation of an input signal with a linearly chirped pump, thereby imparting the necessary quadratic phase modulation required for time lens action. The chirp rate and net bandwidth obtainable with this technique is substantially larger than that obtainable with electro-optic time lenses and should prove useful in further developing finer resolution temporal imaging systems.

## 7. ACKNOWLEDGEMENTS

The authors gratefully acknowledge the support of the National Science Foundation, the ATRI program of the US Air Force, and the David and Lucile Packard Foundation.

## 8. REFERENCES

1. P. Tournois, "Analogie optique de la compression d'impulsion," *Compt. Rend. Acad. Sci. (Paris)*, vol. 258, pp. 3839-3842, April 1964; and *Ann. de Radioélect.*, vol. 19, pp. 267-280, Oct. 1964.
2. A. Papoulis, Systems and transforms with applications in optics, Ch. 1, 6, McGraw-Hill, New York, 1968.
3. S. A. Akhmanov, A. P. Sukhorukov, and A. S. Chirkin, "Nonstationary phenomena and space-time analogy in nonlinear optics," *Sov. Phys. - JETP*, vol. 28, pp. 748-757, 1969.
4. P. Tournois, J-L Vernet, and G. Bienvenu, "Sur l'analogie optique de certains montages électroniques: Formation d'images temporelles de signaux électriques," *Compt. Rend. Acad. Sci. (Paris)*, vol. 267, pp. 375-378, August 1968.
5. W. J. Caputi, "Stretch: A time transformation technique," *IEEE Trans. Aerospace Electron. Syst.*, vol. AES-7, pp. 269-278, 1971.
6. B. H. Kolner and M. Nazarathy, "Temporal imaging with a time lens," *Optics Letters*, vol. 14, pp. 630-632, 1989, and erratum vol. 15, p. 655, 1990.
7. B. H. Kolner, "Space-time duality and the theory of temporal imaging," *IEEE J. Quant. Elect.*, vol. 30, no. 8, pp. 1951-1963, Aug. 1994.
8. B. H. Kolner, "Generalization of the concepts of focal length and  $f$ -number to space and time," *J. Opt. Soc. Am. A*, vol. 11, no. 12, pp. 3229-3234, Dec. 1994.
9. B. H. Kolner, "Active pulse compression using an integrated electro-optic phase modulator," *Applied Physics Letters*, vol. 52, no. 14, pp. 1122-1124, 1988.
10. A. A. Godil, B. A. Auld, and D. M. Bloom, "Time-lens producing 1.9 ps optical pulse," *Applied Physics Letters*, vol. 62, pp. 1047-1049, 1993.
11. M. T. Kauffman, A. A. Godil, W. C. Banyai, and D. M. Bloom, "Applications of time lens optical systems," *Electronics Letters*, vol. 29, pp. 268-269, 1993.
12. A. A. Godil, B. A. Auld, and D. M. Bloom, "Picosecond time-lenses," *IEEE J. Quant. Elect.*, vol. 30, no. 3, pp. 827-837, March 1994.
13. B. H. Kolner, C. V. Bennett, and R. P. Scott, "Space-time duality and temporal imaging," *Proc. SPIE OE/LASE*, vol. 2116, paper #37, 1994.
14. C. V. Bennett, R. P. Scott, and B. H. Kolner, "Up-conversion time lens demonstrates 12x magnification of 100 Gb/s data," *Proc. LEOS Conference*, Paper UO4.2, 1994.
15. C. V. Bennett, R. P. Scott, and B. H. Kolner, "Temporal magnification and reversal of 100 Gb/s optical data with an up-conversion time microscope," *Applied Physics Letters*, vol. 65, no. 20, pp. 2513-2515, Nov. 1994.
16. E. B. Treacy, "Optical pulse compression with diffraction gratings," *IEEE J. Quant. Elect.*, vol. QE-5, no. 9, pp. 454-458, Sept. 1969.
17. C. Fiorini, C. Sauteret, C. Rouyer, N. Blanchot, S. Seznec, and A. Migus, "Temporal aberrations due to misalignments of a stretcher-compressor system and compensation," *IEEE J. Quant. Elect.*, vol. 30, no. 7, pp. 1662-1670, July 1994.